Probe tone thresholds in the auditory nerve measured by two-interval forced-choice procedures

Evan M. Relkin
Institute for Sensory Research and Department of Bioengineering, Syracuse University, Syracuse, New York 13244-5290

Denis G. Pelli
Institute for Sensory Research, Syracuse University, Syracuse, New York 13244-5290

(Received 16 April 1987; accepted for publication 11 August 1987)

An important goal of auditory physiology is to relate the coding of signals in the auditory nerve to behavioral sensitivity. A useful step towards that goal is to measure physiological thresholds for the detection of tones in the neural spike train that are comparable to psychophysical thresholds. Detectability depends on the variability as well as the mean value of the response. A two-interval forced-choice task provides a criterion-free measure of detectability. On each trial of our experiments a probe tone was taken to be correctly detected if the number of spikes in response to the tone exceeded the number of spikes in an otherwise identical interval that did not contain the probe tone. (Analysis of the pulse-number distributions also allowed construction of ROC curves directly comparable to psychophysical ROC curves.) The proportion of trials that yielded correct detections was measured as a function of stimulus intensity to form a *neurometric* function, directly comparable to a psychophysical psychometric function. Threshold was defined as the intensity that produced a given proportion correct. The threshold intensity was also measured by an up–down procedure. Agreement between the two measures of threshold was excellent. Using the up–down procedure we could measure threshold in about 1 min, making it practical to measure the thresholds of a single neuron for many conditions. Comparisons of physiological and psychophysical ROC curves and neurometric and psychometric functions show systematic differences indicating that the animal makes its decisions inefficiently, perhaps by basing its decision on the maximum response among many neurons, rather than just the activity of the single most sensitive neuron.

PACS numbers: 43.63.Pd, 43.63Wj, 43.63.Th, 43.66.Gf

INTRODUCTION

An important goal of sensory physiology is to relate the neural representation of stimuli to the behavioral sensitivity of the animal. The experiments that we describe here result from attempts to relate forward masking in the auditory nerve to forward masking measured psychophysically. Traditionally, neural "thresholds" are defined as the stimulus intensity required to produce a specified increase in an *average* measure of neural response, such as average firing rate or the average degree of synchronization. However, these definitions of threshold ignore the fact that the detectability of a given increase in average response will depend on the *variability* of the response. Existing studies of forward masking in the auditory nerve have only reported the effects of the masker on the average firing rate, and not what effects the masker has on the variability (Smith, 1977, 1979; Bauer, 1978; Harris and Dallos, 1979). Therefore, we have sought to take into account the mean and variance of firing rate and determine what effects the masker has on the detectability of the probe tone, based on the best possible use of the information in a single auditory nerve.

Recently, other methods of measuring neural thresholds in the auditory nerve that take into account the statistical nature of the responses have been reported (Geisler *et al.*, 1985; Sinex and Havey, 1986; Young and Barta, 1986). The methods described in this article differ in that they were designed to be quick and directly comparable to analogous psychophysical methods. Methods analogous to ours have been used to compare visual physiology and psychophysics (e.g., Barlow and Levick, 1969a,b; Barlow *et al.*, 1971; Tolhurst *et al.*, 1983; Parker and Hawken, 1985).

The activity of a nerve fiber provides information about the presence of a probe tone (the signal), generally firing more rapidly when the signal is present. However, to detect the signal, that is, to decide whether or not the signal is present (a *yes–no* task), we should reduce the train of activity to a single number, a *decision variable*, reflecting the likelihood ratio that the signal is present as opposed to being absent, and we would say "yes" if the decision variable exceeds a criterion value and "no" otherwise. That is the ideal way to use any sort of statistical data to detect a signal with the highest possible reliability (Peterson *et al.*, 1956; Van Trees, 1968). We are free to choose any value for the criterion, trading off increases in probability of true positives against increases in the probability of false positives. The disadvantage of the yes–no task is that each subject chooses his or her own criterion in a subjective way, introducing an extra degree of freedom in the results. Note that the subject's deci-

 0001-4966/87/111679-13$00.80

sion-variable criterion is analogous to the physiologist's average-response criterion.

Psychophysicists more and more often now avoid dealing with the criterion by using criterion-free methods, especially the two-interval forced-choice (2IFC) task. We too used 2IFC, both to measure detectability in a way that does not depend on an arbitrary criterion, and to facilitate comparison with psychophysics.

The 2IFC task has two intervals, in random order, one of which contains a signal and one of which does not, but that are otherwise identical. The subject must choose which interval contained the signal. The ideal strategy, resulting in the highest possible reliability, is to base the decision on each interval's *likelihood ratio*, the ratio of the likelihood that the signal is present and the likelihood that the signal is absent. Ideally the likelihood ratio is computed from all available data, and the subject chooses the interval that produced the higher value (Tanner and Swets, 1954). In fact, since the decision variable is only used for relative comparisons, the same ideal level of performance will be attained with any decision variable that is a monotonic transformation of the likelihood ratio.

In theory, the raw data are the set of spike arrival times during each interval. The ideal decision variable would be the likelihood ratio (or any monotonic transformation thereof) computed from these spike trains, but this computation would require more knowledge than we have of the statistics of the spike train. Therefore, we somewhat arbitrarily summarized each spike train by a spike count.

In our experiments we took the spike count over the duration of the signal (with a 2-ms delay; see Sec. I) as the decision variable. This may not be the optimal decision variable, but we believe it is reasonably good. In fact it is not possible, with a finite amount of data, to prove that a given decision variable is optimal without making some assumptions about the underlying statistics of the nerve response. However, it is important to realize that the reliability of detection observed with our suboptimal decision variable does not depend on any assumptions. With an optimal decision variable the thresholds would be even *lower*.

Having noted that the decision variable we used may be suboptimal, it is also worth pointing out that it may be *more* reliable than the animal's or even a human observer's psychophysical behavior. This is because the definition of the decision variable assumes exact knowledge of the signal: the onset and offset times of the signal, and which nerve is carrying the signal, or is most sensitive to it. (We always test at CF, the frequency to which the nerve is most sensitive.) Psychophysical experiments usually cue the subject (e.g., with a light) as to when the signal is on, and often present many trials with the same or similar signals. In principle this gives the subject sufficient information for exact knowledge of the signal. However, it is by no means obvious that subjects are able to effectively use this knowledge to make efficient psychophysical decisions. Indeed, at least in vision, the contrary hypothesis, that the subject acts as though uncertain as to the physical parameters of the signal, offers a unifying explanation of many phenomena (Pelli, 1985).

Thus the performance attained by the decision variable in our study is an approximation to the optimal level of performance that the nerve data could support. This ideal is important because it defines the *highest* level of performance attainable with a single-nerve fiber. However, a psychophysical subject may use the single-nerve data inefficiently and consequently perform less reliably, e.g., by counting spikes over too long or too short an interval. Thus differences in the performance between the (nearly) ideal decision variable used in our study and psychophysical performance will provide evidence about the way that psychophysical subjects use their nerve data to make decisions about the stimulus.

We define *threshold* as the signal intensity required for a given probability of correct detection in the 2IFC task. The most straightforward way to measure threshold is to measure the proportion correct at each of a predetermined set of stimulus intensities. The results are plotted as a "psychometric function," hereafter referred to as the *neurometric function* when based on neural data, as suggested by Movshon *et al.* (1982). This function describes proportion correct as a function of stimulus intensity. Threshold is found by using a smooth curve to interpolate between measured points to estimate the intensity at which the proportion correct equals our chosen value.

However, if one is interested solely in threshold, and not the shape of the psychometric or neurometric function, it is more efficient to use an up–down procedure that uses the results of preceding trials to choose intensities closer and closer to threshold (e.g., Zwislocki *et al.*, 1958; Taylor and Creelman, 1967; Levitt, 1971; Watson and Pelli, 1983). An up–down procedure very similar to ours was used by Delgutte (1987) to study intensity discrimination in the discharge patterns of the auditory nerve of the cat.

I. METHODS

A. Surgical preparation

Chinchillas less than 2 years old were anesthetized with intraperitoneal injections of Dial in urethane (100 mg/ml diallybarbituric acid, 400 mg/ml urethane, 0.55 ml/kg by body weight). Supplemental injections were administered as needed. Body temperature was maintained at 38 °C. During surgery and data collection, the chinchilla's head was warmed by a dc powered, high-intensity lamp. The electrocardiogram and heart rate were monitored as indicators of the physiological condition of the animal. The trachea was cannulated but artificial respiration was rarely necessary. The musculature over the left auditory bulla and the occipital bone was removed. A 0.3-mm hole was drilled in the bulla to allow for equalization of the air pressure in the bulla with ambient air pressure (Guinan and Peake, 1967). The cochlea was visualized through a temporary hole drilled in the dorsal aspect of the bulla. A round window electrode was inserted through this hole and secured with dental cement that also sealed the observation hole. The auditory nerve was approached via the standard dorsal approach. The occipital bone was removed, the underlying membranes were cut away, and portions of the cerebellum were aspirated in order to visualize the auditory nerve at the internal meatus. The left pinna and ear canal were removed to allow for the even-

tual placement of a closed sound-delivery and monitoring system. The animal was then transferred to a double-walled sound attenuating booth.

B. Data collection

After the animal was placed in the sound attenuating booth, the sound delivery system, a Beyer DT-48 transducer in a custom housing, was sealed in the external meatus. A calibrated probe-tube microphone was inserted and sealed in a hole in the lateral wall of the bulla so that its tip was located in front of the tympanic membrane. The sound pressure at the tympanic membrane was measured for 303 frequencies in the range 0.05–22.0 kHz and stored as a computer file.

Compound action potential (CAP) thresholds were determined by visual inspection of the averaged round window response to 32 presentations of a 25-ms tone burst with 2.0-ms cosine-squared ramps. CAP thresholds were measured at 0.5 kHz, and 1.0–10 kHz in 1.0-kHz steps, and 12.0–22.0 kHz in 2.0-kHz steps. Results were compared to average results from several previous studies (Relkin, unpublished data). All data in this report are from chinchillas whose CAP thresholds were within two standard deviations of the averaged normal thresholds for all frequencies. CAP thresholds were monitored periodically throughout the course of the experiments. Data collection was terminated when the threshold at any frequency was more than 10 dB greater than the original threshold.

Single-unit responses in the auditory nerve were recorded with glass microelectrodes (30–100 MΩ filled with 2 M NaCl) advanced into the nerve by a remote control hydraulic, and, in later experiments, a piezoelectric microdrive. A gated, broadband noise was used as a search stimulus. After contact with a neuron was established, the peristimulus time histogram (PST) in response to a click was recorded. Latency was measured as the time delay to the first peak of the PST. Latency was the principal means of identifying neurons as primary (Kiang *et al.*, 1965). The spontaneous activity of the neuron was monitored for 20 s. A frequency threshold curve (FTC) was then measured for the middle 50 ms of the response to 75-ms tone bursts. For the FTC, threshold was defined as the intensity that increased the spike count during the 50 ms by 2. The method for measuring the FTC was similar to that described by Kiang *et al.* (1970). The computer program displayed the FTC in real time and calculated and displayed the characteristic frequency (CF), threshold at CF, and the relative 10-dB bandwidth, $Q_{10\ dB}$. If the FTC appeared abnormal, CAP thresholds were measured at several frequencies as soon as contact with the neuron was lost to check for physiological deterioration of the auditory periphery.

1. Stimulus timing and spike counts

All stimuli used in these experiments were gated pure tones with a frequency equal to the CF of the respective neuron. Figure 1 shows the timing of the electrical signals used to generate the stimulus for one 2IFC trial. The probe was randomly presented either in interval 1 or in interval 2. Probe tones were 25 ms in duration, including the gating on and off by 2-ms cosine-squared ramps. This probe tone duration was chosen to be similar to that used in psychophysical experiments with chinchillas (Halpern, 1985; Halpern and Dallos, 1986) and to be short enough to minimize the complicating effects of post-stimulatory recovery during the response to the probe. Masking tones were 102 ms long with the same onset and offset ramp parameters as the probe tone. Zero time delay between the masker and the probe tone was defined as the case when the end of the masker offset ramp coincided with the beginning of the probe tone onset ramp. The time between presentations of the masker was 400 ms. The spike-counting intervals were delayed by 2 ms to allow for the latency of the neural response.

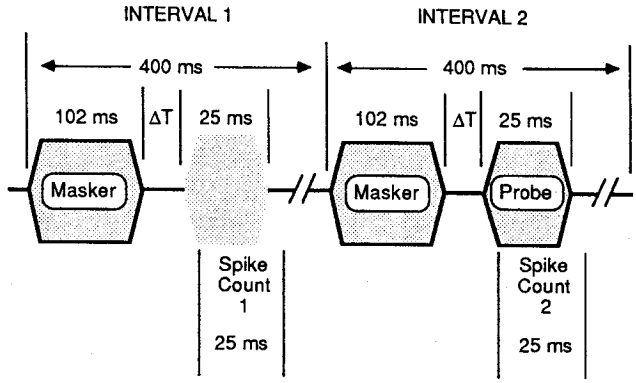

FIG. 1. Timing of the electrical signal used to generate the stimuli. All ramps were 2-ms cosine squared. The probe was randomly presented either in interval 1 or in interval 2. Spike counting intervals were delayed 2 ms relative to the electrical stimulus to allow for the latency of the neural response.

We used the spike count as the decision variable. The above definition of the spike-counting interval was made after examining PST histograms (which show the average response over time) at several probe intensities and delays between masker and probe. The counting interval that we chose includes most of the probe response, and little of the masker response. Of course, the ideal decision variable (for highest 2IFC proportion correct) would not use a simple counting interval that weighs all spikes equally, but would instead weigh incoming spikes according to the signal-to-noise ratio (averaged over many similar trials) prevailing at the time of arrival. However, such a decision variable would use a different weighting function for each condition, which was beyond the scope of this study.

Average firing rate during both masker intervals was measured to determine the firing rate in response to the masker, or, in the case of there being no masker, the spontaneous activity. For long recordings from a single neuron these measures were useful for monitoring the stability of the recording. In particular, it was possible to check for fatigue which might result from high-intensity maskers.

If the number of spikes counted with the probe present exceeded the number of spikes counted in the equivalent time period in the other interval, the probe was considered to be correctly detected. If the counts were equal, the number of correct detections of the probe was incremented by 0.5 since any choice of interval would, on average, be correct on 50% of the trials.

2. Experiment I: Neurometric functions

Neurometric functions were determined from the results for 50 trials at each intensity. Since each trial required 800 ms, 40 s were required to determine the probability of detection at each intensity. The proportion correct was taken as the number of correct detections of the probe divided by the total number of trials. Upon completion of the 50 trials, the proportion correct and the average firing rate during the masker interval were calculated, displayed on the computer terminal, and printed on a continuous record of the experiment. The initial intensity tested was chosen to be several decibels below the threshold determined using the up–down procedure. If the proportion correct at this intensity was not approximately 50% then lower intensities were tested. Intensity was then increased in 2-dB steps until several intensities were tested that yielded proportions correct close to 100%. While measuring the 2IFC proportion correct, pulse-number distributions (Teich and Khanna, 1985; Westerman, 1985; Young and Barta, 1986) were collected and stored for the spike counts in each of the two intervals.

Analysis of the neurometric functions was enhanced by a maximum likelihood fit of a Weibull function (Eq. 1, Weibull, 1951) to the data (see Watson, 1979, for methods). The Weibull function has well-established general utility for fitting psychometric data (Quick, 1974; Green and Luce, 1975). The use of the fitted function was particularly important because of the modest number of trials (50) at each stimulus level. The number 50 was chosen to make it possible to collect complete neurometric functions during the average holding time of a single neuron. Note that the Weibull function is fitted to all the trials at all intensities, not just the 50 trials at any one intensity. The Weibull function is

$$P(I) = 1 - 0.5e^{-(I/I_{0.82})^{\beta}}, \qquad (1)$$

where we have fixed the "guessing rate" parameter at 0.5 since we are fitting 2IFC data, P is the probability of correct detection, I is the intensity of the signal, $I_{0.82}$ is the intensity of the signal at which $P = 0.82$, and β determines the slope of the function. The FORTRAN program QUICK 2 (derived from QUICK, Watson, 1979) was used to calculate maximum likelihood estimates for the parameters $I_{0.82}$ and β. The program also calculated the significance level p, based on chi-square statistics, at which the fit could be rejected. (The significance level p is the probability, if the model is correct, that the data would deviate by at least as much as observed.)

Examples of calculated Weibull functions are shown in Fig. 2 for several values of β. The units for the abscissa are normalized intensity $I/I_{0.82}$ expressed in decibels. Notice how β determines the slope of the function. Readers wishing to compare our slopes with those of psychometric functions may wish to note that the slope of the Weibull function $P(I)$ in percent correct per dB at the point $I = I_{0.82}$ is 4.24β %/dB.

3. Experiment II: Up–down procedure

The procedure for converging on a fixed level of performance by adaptive adjustment of probe tone intensity was adapted from the PEST procedure (parameter estimation by sequential testing, Taylor and Creelman, 1967). Specifically, we used the PEST rules for determining increments and decrements of attenuation, so as to converge on threshold. As intensity converges on threshold, the attenuator step size is decreased. When the step size is reduced to some predetermined minimum, in this case 0.5 dB, the up–down sequence is taken to have converged and the final intensity is taken as threshold. Each sequence was begun at maximum attenuation with an initial step size of 16 dB. In our modification of the PEST procedure, we continued running after the minimum step size was reached, until three reversals occurred at the minimum step size. Threshold intensity was taken as the average of the intensities at the three reversals.

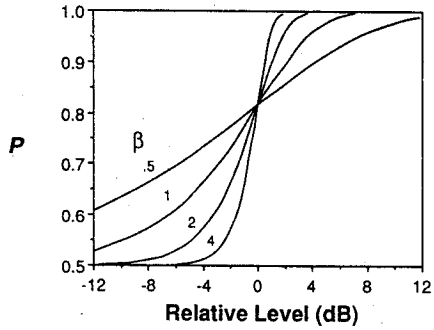

FIG. 2. Weibull functions. The probability of correct detection P is plotted as a function of relative amplitude $I/I_{0.82}$ expressed in decibels. The slope parameter β of each curve is indicated on the figure.

Contrary to PEST, the decision to increase or decrease intensity was based on four trials. If the total number of correct detections of the probe tone was three or more, the intensity was decreased; otherwise it was increased. The up–down sequence converges on an equilibrium intensity, hopefully threshold, at which the average change in intensity is zero, so the probability of an increase is 0.5 (and the probability of a decrease is 0.5 too). The probability P of a correct detection for a *single* trial at this level of performance (based on *four* trials) can be calculated by solving the following equation from binomial statistics:

$$0.5 = P^4 + 4P^3(1 - P). \qquad (2)$$

Solution of this equation yields $P = 0.61$. Therefore, threshold determined by this up–down procedure should approximate the intensity at which the neurometric function equals 0.61. In fact, we found empirically, as will be explained below, that the average of the up–down thresholds was equal to the intensity at which $P = 0.66$.

Occasionally, this method yielded final reversals that were many decibels apart, suggesting that the method had not converged. These suspect threshold estimates were averaged with repeat measurements.

II. RESULTS

A. Experiment I

Neurometric functions were measured in three animals. Thirty complete intensity functions for unmasked, and masked, conditions were obtained for 21 primary auditory neurons. The neurometric functions exhibit the usual sigmoid shape observed for psychometric functions. Typically, the proportion correct increases from 50%–100% over a 24-

dB range of intensity. Using 2-dB increments, measurements were made at 12 points in a total time of 8 min.

Figures 3(a), 4(a), and 5(a) are examples of neurometric data, with best-fitting Weibull functions, under conditions of no masking for two high spontaneous rate fibers [Figs. 3(a) and 4(a)] and one low spontaneous rate fiber [Fig. 5(a)]. None of the fits for the data reported here could be rejected (significance $p > 0.16$). (One fit was rejected at significance $p = 0.03$. The poor fit was probably a result of the poor stability of the preparation as indicated by the measurement of spontaneous rate during each trial.)

The shape of the neurometric functions, as measured by β of the Weibull function, was very consistent and averaged 1.10 [standard deviation (s.d. = 0.36)] for unmasked conditions and 1.04 (s.d. = 0.34) with forward masking conditions. The average is 1.07, corresponding to a slope of 4.6%/dB at the point where $I = I_{0.82}$. β is plotted in Fig. 6 for all complete intensity functions versus spontaneous rate. The slope seems to be independent of spontaneous rate at all but perhaps the lowest rates, for which the slope appears to be greater, but there are too few data points to be sure. Slopes obtained under conditions of forward masking are plotted as filled symbols, and appear to be the same as the slopes obtained with no masking, which are plotted as open symbols. More will be said about this in a second article (Relkin and Turner, in preparation).

Examples of the pulse-number distributions for an intensity near threshold ($P \approx 0.61$) and for an intensity that produced almost perfect performance ($P > 0.97$) are shown in parts (c) and (d) of Figs. 3–5. Each plot shows both the response distribution for the no-probe interval (open symbols) and the probe interval (closed symbols). Notice the small but consistent differences between the two distributions when the probability of detection is close to 0.61 and the much larger differences between the distributions when the probability of detection approaches 100%. For instance, in Fig. 4(c), the mean number of pulses for the two distributions when $P = 0.61$ is 1.74 for the no-probe condition and 2.14 for the probe condition. Notice that the two distributions are similarly shaped, differing primarily in the shift to the right to higher spike counts.

The pulse-number distributions can be further analyzed computing a receiver operating characteristic (ROC) by integrating the appropriate areas under the pulse-number distribution (Green and Swets, 1966). ROC curves for the response to the probe tone are plotted in part (e) of Figs. 3–5 for the two conditions plotted in parts (c) and (d). The vertical scale is the probability P_{SN} of a true positive, i.e., the

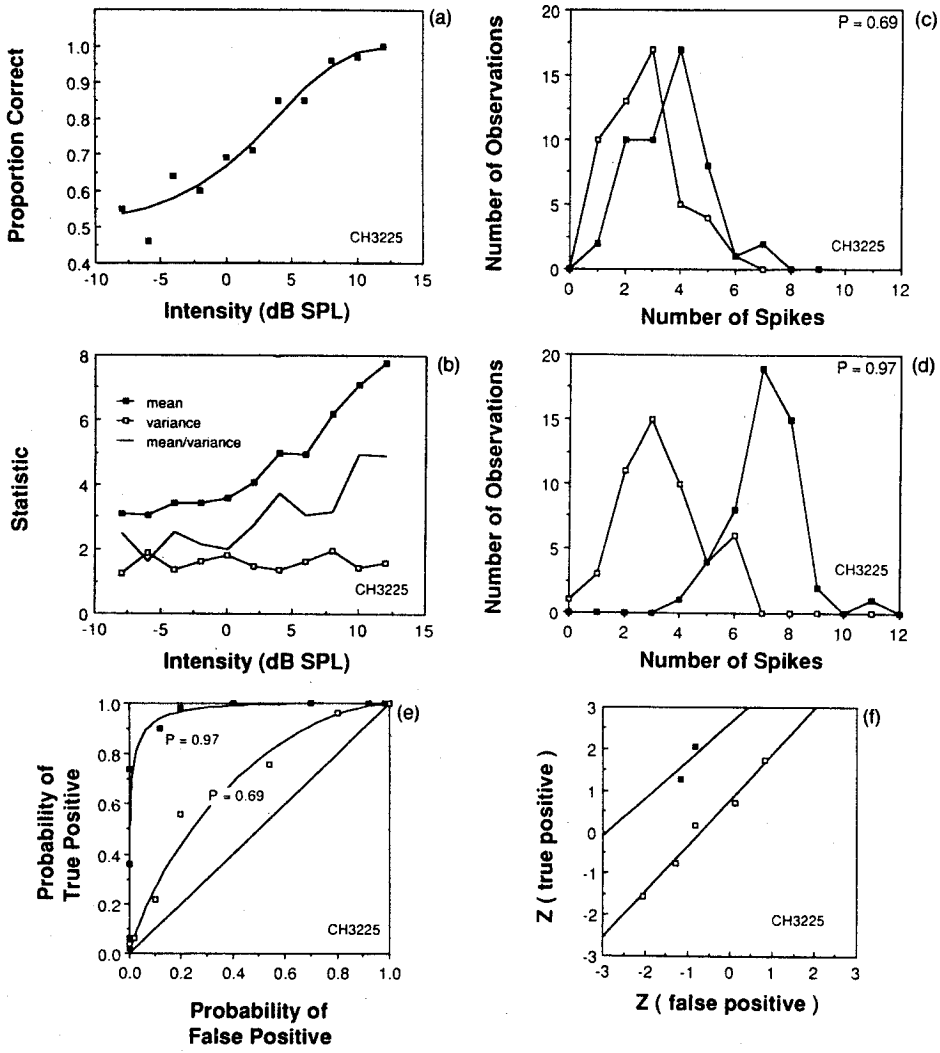

FIG. 3. Data derived from the measurement of the neurometric function for one fiber with spontaneous rate of 118.6 spikes/s; CF = 3357 Hz. (a) The neurometric function is plotted as a function of probe tone intensity. The solid symbols are the experimental data and the solid line is the fitted Weibull function. (b) The mean, variance, and ratio of mean to variance are plotted versus intensity for the response to the probe for all points of the neurometric function. (c) The pulse-number distribution is plotted for an intensity near the threshold determined by the up–down procedure. The probability of correct detection P is indicated on the figure. Open symbols are for the no-probe interval and closed symbols are for the probe interval. (d) Similar to (b), but for an intensity that resulted in a probability of detection near 100%. (e) Receiver operating characteristics for the two conditions of panels (c) (open symbols) and (d) (closed symbols). The solid curve is the best fit of the unequal-variance Gaussian model to the data. (f) The same data and curves from panel (e) are replotted on double probability axes.

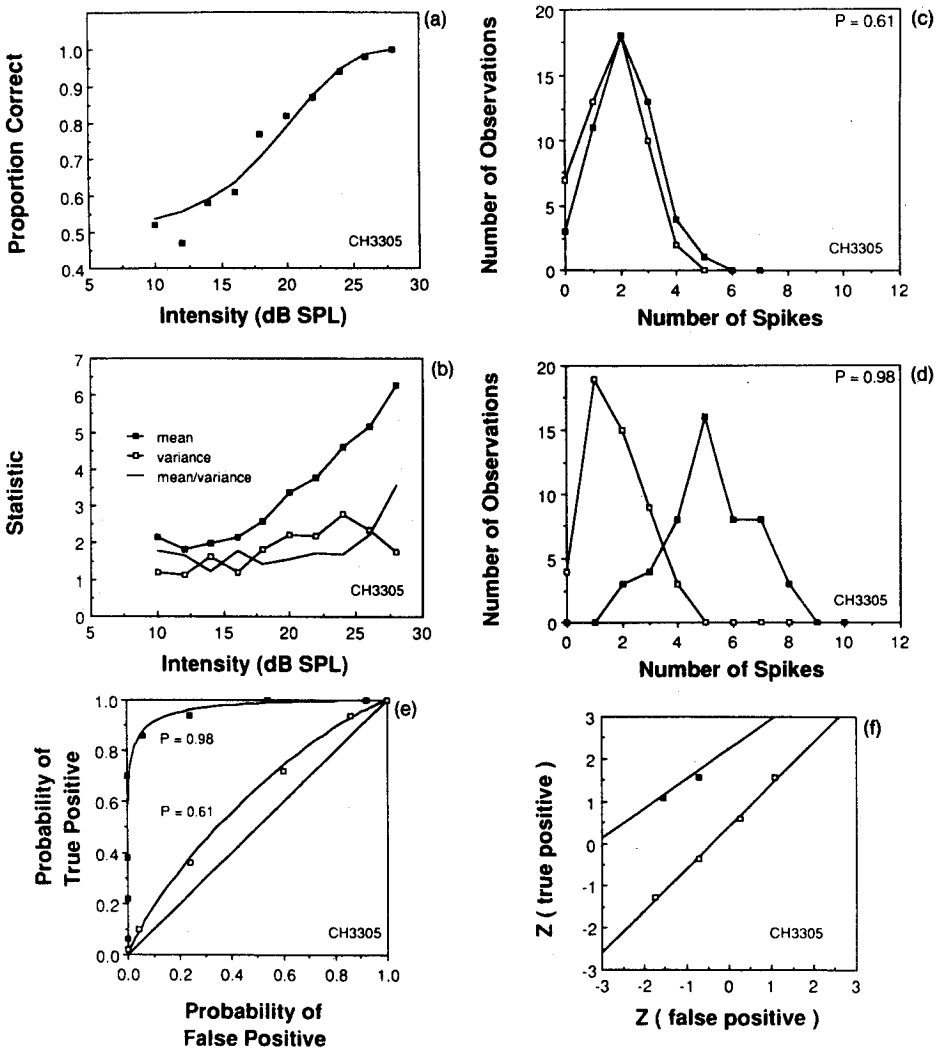

FIG. 4. Same as Fig. 3, for a neuron with spontaneous rate of 58.8 spikes/s; CF = 2911 Hz.

probability of exceeding a criterion spike count λ on a probe interval. The horizontal scale is the probability P_N of a false positive, i.e., the probability of exceeding λ on a no-probe interval. The subscripts SN and N are traditional, and stand for "signal plus noise" and "noise only," respectively. Given some mild assumptions (e.g., stationarity) and a sufficiently large sample, the area under the ROC curve is equal to the probability of correct detection in a 2IFC trial (Green and Swets, 1966). The area between the ROC curve and the diagonal line gives the improvement in performance above chance, i.e., $P = 0.5$. Notice that even for the conditions where the difference between the pulse-number distributions for the probe and no-probe conditions appears to be very small [compare Fig. 4(c) and (e)], the corresponding ROC curve clearly shows that performance is above chance.

The ROC curves in Figs. 3(e) and 4(e) may be replotted on double-probability axes, as shown in Figs. 3(f) and 4(f), transforming the probabilities P_{SN} and P_N to normal deviates z_{SN} and z_N. A normal deviate z is related to a probability P by the cumulative normal integral,

$$P = \frac{1}{\sqrt{2\pi}} \int_{-\infty}^{z} e^{-u^2/2}\, du, \tag{3}$$

which is tabulated in most elementary books on statistics. It is a common empirical finding in many disciplines that ROC curves become straight lines in the double-probability coordinates z_{SN} vs z_N (Swets and Pickett, 1982). Happily that was true for our data as well. This allows us to summarize each curve by the parameters of the best-fitting line, as shown in Figs. 3(f) and 4(f).

The straight-line fits can be interpreted as the parameters of an unequal variance Gaussian model. Readers unfamiliar with ROC analysis should not be alarmed by the use of a Gaussian model to fit the neural ROC data. We know the spike counts are not Gaussian. (Although, by the central limit theorem, a Poisson distribution with large mean is asymptotically Gaussian.) We use the unequal-variance Gaussian model because it is the traditional way to summarize ROC data, particularly psychophysical data, and we wish to compare the properties of our neural ROC curves with those of traditional psychophysical ROC curves. This approach is operational. The Gaussian model predicts straight lines in double probability space. Our data form approximately straight lines. It is traditional to use the Gaussian model to extract the height and slope of those lines.

The fits were made by the computer program RSCORE (Dorfman and Alf, 1969; Swets and Pickett, 1982), which finds the parameters of an unequal-variance Gaussian model to provide a maximum likelihood fit to the ROC data. The parameters of the Gaussian model are explained in Appen-

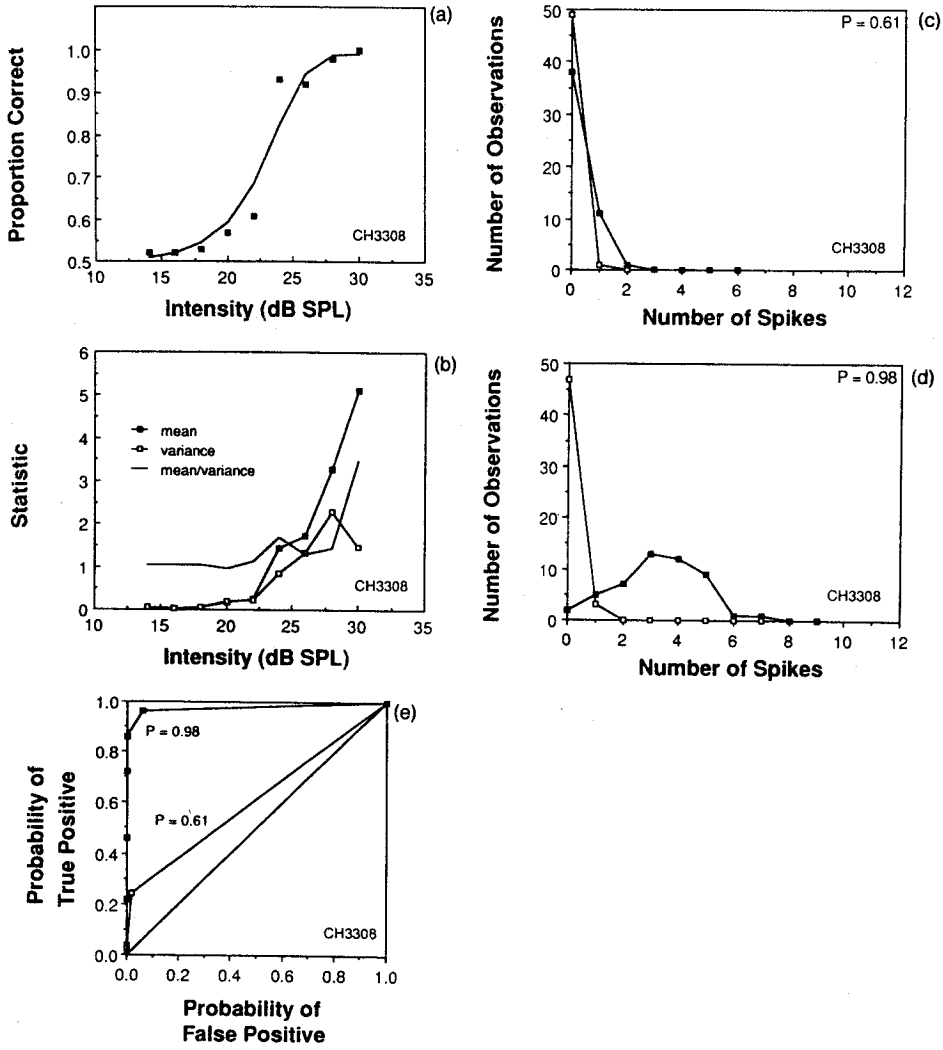

FIG. 5. Same as Fig. 3, for a neuron with spontaneous rate of 1.1 spikes/s; CF = 4213 Hz. In panel (e) the solid line simply connects the points. The unequal-variance Gaussian model could not be applied to low spontaneous rate neurons as explained in the text. For the same reasons, panel (f) is omitted.

dix A. A chi-square test could not reject any of the fits to the ROC curves. However, we had to reject the fits to the data from the low spontaneous neurons (firing rates less than 1 per second) such as the one in Fig. 5. These neurons have a classical high threshold, yielding nonzero spike counts very rarely unless the probe is present. When a spike does occur it is very strong evidence of the probe's presence. As a result, the ROC curves have only one point for which both true and false positive rates are nonzero and less than 1. A single point is not enough to determine the slope of a line, so we were forced to discard these fits even though they passed the chi-square test.

Each fit is a line, and has two parameters: Δm, the negative horizontal intercept with the z_N axis, and s, the slope (Green and Swets, 1966),

$$z_{SN} = s(z_N + \Delta m). \tag{4}$$

In human psychophysics, the slope s may be 1 or less than 1, depending on conditions and on the subject (Green and Swets, 1966). When the slope is less than 1 it is often found that the parameters Δm and s are related by the empirical formula $\Delta\sigma/\Delta m \approx 1/4$, where $\Delta\sigma = 1/s - 1$ (Green and Swets, 1966; Nachmias and Kocher, 1970).

Table I shows the parameters of the ROC fits for the ROC data shown in Figs. 3 and 4. Note that, as expected, the area under the ROC fit agrees with the observed proportion correct. For these four ROC fits the slope s is not significantly different from 1, and the $\Delta\sigma/\Delta m$ ratio is approximately 0, not 1/4. In other words, in the Gaussian model that best fits these ROC curves the variance of the decision variable was approximately equal on signal-plus-noise and noise-only presentations; i.e., the variance was constant, independent of the signal. Since this is of some theoretical significance we applied the same analysis to all our neurons, for moderately

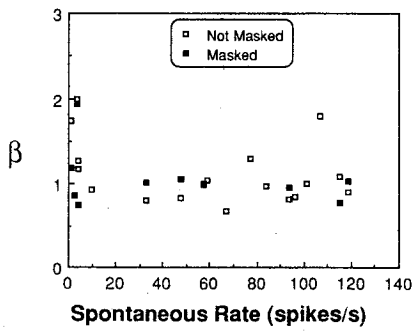

FIG. 6. The parameter β of the fitted Weibull functions is plotted as a function of the spontaneous rate for all completed neurometric functions with acceptable Weibull fits. Open symbols are for unmasked conditions and closed symbols are for forward-masked conditions in which the masker was intense enough to saturate the firing rate.

TABLE I. Parameters of the ROC fits in Figs. 3 and 4. The 2IFC P column is the proportion correct in 50 2IFC trials. The other data columns show the results of a maximum likelihood fit by a Gaussian model (see Sec. II for details). The standard deviations are supplied by the fitting program. The ROC *area* column is the area under the ROC fit, which in theory should (and does) agree with the 2IFC proportion correct P. The Δm and s columns are the negative horizontal intercept and slope of the linear fit. The last column is a derived quantity, where $\Delta\sigma = 1/s - 1$. All computations were done with higher precision, but only the significant digits are shown.

Figure	Neuron	2IFC P	ROC			
			Area	Δm	s	$\Delta\sigma/\Delta m$
3	CH3225	0.69	0.70 ± 0.05	0.6 ± 0.2	1.2 ± 0.2	-0.2 ± 0.2
		0.97	0.98 ± 0.01	3.1 ± 0.7	0.8 ± 0.3	0.1 ± 0.2
4	CH3305	0.61	0.61 ± 0.06	0.4 ± 0.2	1.0 ± 0.2	0.1 ± 0.5
		0.98	0.97 ± 0.02	3.2 ± 0.8	0.7 ± 0.2	0.2 ± 0.2

detectable ($0.59 \leqslant P \leqslant 0.76$) and highly detectable ($0.85 \leqslant P \leqslant 0.99$) probe intensities.

Table II shows the average results. The table legend explains why some ROC fits could not be included. When the probe was moderately detectable ($0.59 \leqslant P \leqslant 0.76$), the slope s was not significantly different from 1. However, when the probe was highly detectable ($0.85 \leqslant P \leqslant 0.99$), the average slope was 0.76, and significantly less than 1. The derived parameter $\Delta\sigma/\Delta m$ did not differ significantly between the two groups, and had an overall average of 0.08, significantly less than the traditional value of $1/4 = 0.25$. Thus we find that the ROC data are compatible with a Gaussian model in which the variance grows slowly with the signal strength. However, this refers solely to the parameters of a Gaussian model fit to the ROC data. The ROC data reflect only the detective power of the decision variable, and not all of its underlying properties. It is of interest, therefore, to directly examine the mean and variance of the decision variable.

The mean number of spikes, variance, and ratio of mean to variance calculated from the pulse-number distributions are plotted as functions of intensity for each neuron in Figs. 3(b), 4(b), and 5(b). As expected, the mean number of spikes increases with intensity. The behavior of the variance is complicated, varies from neuron to neuron, and seems to depend on spontaneous rate. The ratio of mean to variance reflects this complexity. At low levels the variance increases with level, but more so for low spontaneous rate neurons [Fig. 5(b)]. For some very high spontaneous rate neurons the variance has been observed to be almost constant with level [Fig. 3(b)]. At very high levels the rate of increase of the variance decreases, and in some cases the variance itself decreases [Fig. 4(b)]. The net result is that the ratio of mean to variance can become very much greater than 1 at high levels. We have observed ratios as high as 6.

TABLE II. Average parameters and standard errors of the fits to the ROC curves. P is the proportion correct in the 2IFC trials in which the pulse-number distributions were collected. The data have been grouped into low and high values of P; n is the number of ROC curves that were fit. Δm and s are the minus x intercept and slope of the linear fit (see Sec. II for details). $\Delta\sigma/\Delta m$ is a derived quantity (derived *before* averaging), where $\Delta\sigma = 1/s - 1$. This chart includes the results from all neurons except that we included no more than two ROC fits for each neuron (preferably with values of P near 0.6 and 0.9), low spontaneous rate neurons (less than one spike per second) could not be meaningfully fit, and two ROC fits were excluded as outliers because of extraordinarily large parameter values: One had $s = 2.6$; one had $\Delta m = 20$. In all cases the area under the ROC fit was not significantly different from the measured proportion correct P. The goodness of fit was also evaluated by a chi-square test. Two fits had significance values slightly below 0.05, but the number of such deviations was no more than would be expected by chance (i.e., 1 out of 20) if the underlying model were true, so these fits were included in the analysis.

P	n	Δm	s	$\Delta\sigma/\Delta m$
$0.59 \leqslant P \leqslant 0.76$	22	0.6	0.97 ± 0.03	0.05 ± 0.08
$0.85 \leqslant P \leqslant 0.99$	11	3.1	0.76 ± 0.06	0.12 ± 0.03
$0.59 \leqslant P \leqslant 0.99$	33	1.5		0.08 ± 0.06

B. Experiment II

The up–down procedure was used in experiments with eight animals, three of which included measurements of the neurometric function. In one typical neuron, for which 29 thresholds were determined, the average number of trials per threshold was 81 (s.d. = 31), approximately 1.5 times the number of trials required to measure a single point of the neurometric function. The average number of reversals for this neuron was 11.7 (s.d. = 3.1). Convergence of the up–down procedure was excellent, with the final three reversals usually agreeing within 2 dB.

The validity of the up–down method depends on its ability to determine correctly the intensity at which the neurometric function equals a fixed proportion correct. Up–down thresholds were measured for all of the conditions for which neurometric functions were measured in experiment I. For some neurons, measurements were made in the presence of a forward masker at CF, which produced a saturated average firing rate (Relkin and Turner, 1987; Relkin and Turner, in preparation). In Fig. 7, the threshold determined with the up–down procedure is plotted against threshold determined from the point at which the neurometric function equals 0.61. The agreement between the two measures of threshold (in dB) is very good, with a correlation coefficient of 0.97. The difference in decibels has a mean of 1.7 dB and a standard deviation of 2.7 dB. For a typical β of 1.1, the 1.7 dB higher threshold of the up–down procedure implies that it estimates, on average, the intensity at which $P = 0.66$, rather than 0.61 as we calculated for the equilibrium point.

Figure 8 shows the threshold measured with the up–down procedure plotted against the spontaneous rate of the neuron. There is a gap in the distribution of spontaneous rate at 20 spikes per second similar to that reported by Liberman (1978) in the cat, separating low and medium spontaneous

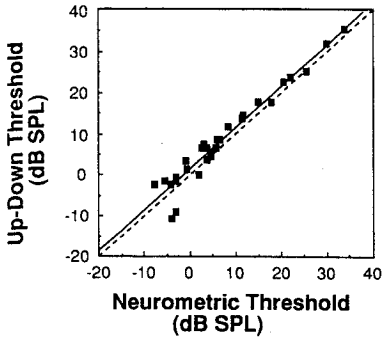

FIG. 7. The 2IFC threshold determined by the up–down procedure is plotted against the 2IFC threshold determined from the neurometric data (the intensity at which the best-fitting Weibull function equals 0.61). A linear regression line (with respect to the intensities in decibels) is plotted on the figure ($R = 0.97$, slope = 1.01). The dashed line indicates equality.

firing rates from high spontaneous rates. Because of the modest number of data points, the low and medium spontaneous rate fibers will be treated as a single class. The low and medium spontaneous rate fibers appear to have higher average thresholds.

Table III shows the average 2IFC threshold (determined by the up–down procedure) and the average FTC threshold for the two classes of neurons at CF. The reader will recall that the FTC threshold is based on an average response criterion of two extra spikes in a 50-ms test interval. Since CF thresholds are relatively constant in the chinchilla (Salvi *et al.*, 1982; Relkin, unpublished data; also, see the lower panel of Fig. 8) for most of the neurons included in this study (1.0 kHz < CF < 14.0 kHz), it is reasonable to average thresholds across all fibers. By either measure, 2IFC

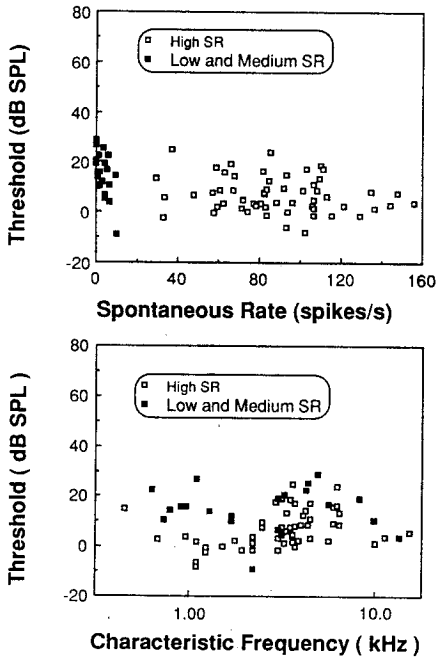

FIG. 8. The 2IFC threshold (determined by the up–down procedure) is plotted as a function of spontaneous rate (upper panel) and characteristic frequency (lower panel). These data are grouped from experiments on several chinchillas. Closed symbols are for neurons with low and medium spontaneous firing rates (SR < 20) and open symbols are for neurons with high spontaneous firing rates (SR > 20).

TABLE III. Comparison of statistics of neural thresholds defined by a 2IFC task (measured by the up–down procedure) with thresholds defined by a criterion increment in the average response [measured by the frequency threshold curve (FTC)]. All thresholds were measured at CF; n is the number of neurons of each type. Each table entry shows mean ± standard deviation, except the differences that show the mean ± standard error. The neurons are grouped into classes based on spontaneous firing rate (SR): low and medium spontaneous rate fibers (SR < 20) and high spontaneous rate fibers (SR > 20). Both differences are significant ($p < 0.001$, Student's t test).

			Threshold at CF	
	SR	n	2IFC	FTC
Low and medium spontaneous rate	< 20	21	14.9 ± 8.8 dB	17.4 ± 8.0 dB
High spontaneous rate	> 20	56	7.0 ± 7.3 dB	6.6 ± 7.3 dB
Difference			7.9 ± 2.9 dB	10.8 ± 2.0 dB

or FTC, low and high spontaneous rate fibers have significantly different thresholds (by Student's t test). The difference in 2IFC thresholds for the two classes is similar to the 5-dB difference reported by Geisler *et al.* (1985) for statistically defined thresholds in the cat. The average FTC threshold for the low spontaneous rate fibers is less than that reported by Liberman (1978) but is consistent with data from other studies in the chinchilla (Salvi *et al.*, 1982; Relkin, unpublished data). Part of the disagreement may be due to differences in the two species and also due to the grouping of low and medium spontaneous rate fibers into one class. Also, we may have missed very high threshold fibers because we did not use an electric shock search stimulus such as used by Liberman. Nonetheless, the current data show that the difference between the thresholds for high and low spontaneous rate fibers is less when threshold is defined in terms of detectability than when threshold is defined in terms of absolute rate increments. In this regard, the data from this study are in good agreement with the study by Geisler *et al.* (1985).

III. DISCUSSION

Young and Barta (1986) also used signal detection theory to measure neural thresholds. They assume that the underlying neural process is a Poisson process with deadtime. They consider two models. In one model the deadtime is constant and in the other model each deadtime is a random sample from an exponential distribution. For each animal they found the model that best fit the spontaneous and continuous-noise-driven activity. When the signal was presented, instead of measuring the response variance, they assumed the variance grew with the mean in the way predicted by the model and they transformed the mean response to make the predicted variance of the response equal to 1. Threshold was taken to be the intensity that produced a unit transformed response. The assumptions of their method contrast with the assumption-free nature of our method for measuring threshold.

Neurometric functions for 2IFC detection of probe tones in the auditory nerve are qualitatively similar in all respects to analogous auditory psychometric functions.

They can be well represented by the Weibull function, which is often used to fit psychometric data. Very limited psychometric data are available for the chinchilla. We have found two examples of yes–no psychometric functions for the chinchilla (Nelson *et al.*, 1976; Halpern, 1985). Unfortunately, we cannot meaningfully compare slopes of their yes–no data with our 2IFC data because the slopes of yes–no psychometric functions depend on the (unknowable) subjective criterion of each animal (Green and Swets, 1966).

Watson *et al.* (1972) have published psychometric functions for the detection of 150-ms tone bursts by human listeners. For probe tone frequencies above 1 kHz the slopes of the psychometric functions were constant. A Weibull function was fit to psychometric data for tones of 1 and 2 kHz from Fig. 2 of the article by Watson *et al.* The β calculated for this function was 2.2 (9.1%/dB) or almost two times greater than the value measured for the chinchilla neurometric functions. A similar finding was presented by Tolhurst *et al.* (1983) for the comparison of neurometric functions for neurons in the visual cortex of monkeys and cats to psychophysical data from humans. In their study the psychophysical β was 2.3 times greater than the physiological β. Tolhurst *et al.* suggested that the difference can be resolved by assuming that the psychophysical slopes reflect decisions based on the combined activity of a small number of neurons.

We also compared the physiological ROC curves with psychophysical ROC curves. The most useful summary is the ratio $\Delta\sigma/\Delta m$, which describes the rate at which the variance of the decision variable grows with the decision variable's mean in the Gaussian model used to fit the results. As reported in Table II, our neurons yielded an average value for $\Delta\sigma/\Delta m$ of 0.08 ± 0.06, which is significantly less than the traditional value of 0.25 found in human psychophysics. Hack's (1963; discussed in Green and Swets, 1966) psychophysical ROC curves for detection of a 2-kHz, 2-s tone by the rat have average ratios $\Delta\sigma/\Delta m$ of 0.41 ± 0.08, which is somewhat higher than the traditional value of 0.25 found in human psychophysics. (The average and $\pm$ standard error is computed from their published results.) Human psychophysical ROC curves for binaural detection of a tone in a white Gaussian noise background have average ratios $\Delta\sigma/\Delta m$ of 0.31 ± 0.08 (for a 1-kHz, 100-ms tone; calculated from condition 1 of Markowitz and Swets, 1967) or 0.23 ± 0.05 (for a 400-Hz, 250-ms tone; calculated from condition NO-SO of Emmerich, 1968), both of which are consistent with the traditional value of 0.25.

The psychophysical data are not adequate for a critical comparison, but they suggest that the decision variable based on a spike count in one neuron yields neurometric intensity functions with shallower slopes β than found psychophysically and ROC curves with slopes s nearer 1 than found psychophysically. However, an animal could use several neurons to make its decision, or could examine responses from a single neuron at several times. Such decisions would reflect a decision variable that was the combination of several like the one we used. Perhaps the simplest combination rule is "probability summation," in which the animal makes an affirmative response whenever any of several monitored responses exceeds the animal's subjective criterion. This is equivalent to saying that the animal's decision variable is the maximum of several responses. This is a nearly ideal way to detect one of many possible signals, i.e., where the signal may arrive by any one of the various monitored neurons or times (Green and Swets, 1966; Nolte and Jaarsma, 1967; Nachmias and Kocher, 1970; Pelli, 1985). Nachmias and Kocher use this model to explain an ROC slope of less than 1. Pelli shows that the same model explains a high slope β of the psychometric function. Thus probability summation might explain both effects. However, one would need psychophysical data on the chinchilla for comparable experimental conditions to draw any firm conclusions.

We examined the mean and variance of the pulse-number distributions for the neural response to short tone bursts. Previous studies have examined these statistics for 51.2-ms samples of the response to continuous tones (Teich and Khanna, 1985) and to 200-ms samples of spontaneous activity and the response to continuous broadband noises (Young and Barta, 1986). Both studies found that the ratio of mean to variance can be greater than 1, indicating that the underlying process cannot be purely Poisson. Teich and Khanna report that this ratio can be as great as 2 but rarely larger. From Fig. 6 of the article by Young and Barta it can be estimated that they measured ratios as large as 3.5. The data of Delgutte (1987; Fig. 6) shows that the ratio can be as great as 4 for 50-ms tone bursts. For the response to 25-ms tone bursts we have seen ratios as large as 6. Westerman (1985) measured the pulse-number distribution for consecutive 5-ms segments of 300-ms tone bursts. He found that the ratio of mean to variance is greatest near the onset of the tone burst, with values as great as 4. The increased ratio for short tone bursts, and for the early segments of longer tone bursts, is the result of the orderliness of the first few spikes in the neural response at high intensities (Goldstein and Kiang, 1958; Özdamar and Dallos, 1978; Lütkenhöner and Smith, 1986). This orderliness results in a decreased variance and, therefore, an increased ratio of mean to variance. Thus shorter tone bursts tend to produce higher ratios of mean to variance.

Eric Young (personal communication) kindly pointed out to us how our data could be used to test the two Poisson models presented by Young and Barta (1986). Each of the models has two parameters, one fixed and one free. In both models the fixed parameter is the duration of the observation interval, which in our experiments was equal to the total duration of our tone bursts, 25 ms. For the constant-deadtime model, the free parameter is equal to the value of the deadtime. For the exponentially distributed deadtime model, the free parameter is the reciprocal of the average deadtime, which is equal to the maximum firing rate (see Young and Barta, 1986, for details). The two models were fit to our data by calculating values of the free parameters that minimized the mean-square error of predicted variance at all mean rates. Examples for two neurons are shown in Fig. 9, where variance is plotted as function of the mean count for the 25-ms observation interval. For neuron CH3305, the best-fitting constant-deadtime parameter was 1.7 ms and the

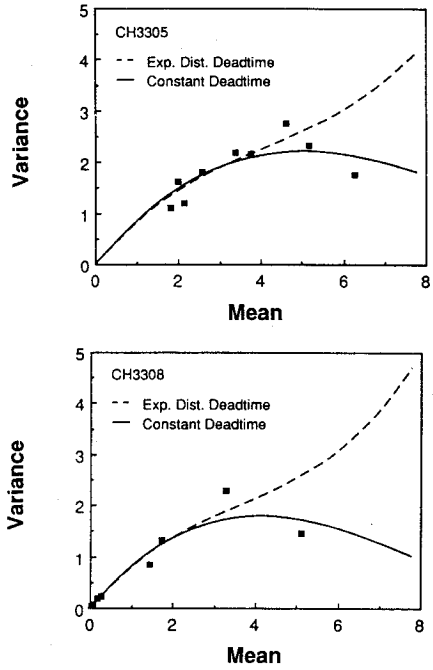

FIG. 9. The variance of the count observed in a 25-ms interval is plotted as a function of the mean for the two neurons of Figs. 4 and 5. The solid and dashed lines are the least-squares fit to the data for a Poisson process with constant deadtime and a Poisson process with exponentially distributed deadtime, respectively. Note that only the constant deadtime model is consistent with the decrease in variance observed at high mean counts.

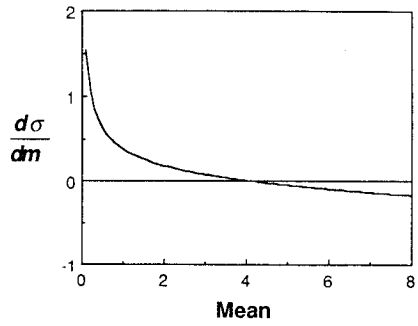

FIG. 10. The derivative $d\sigma/dm$ is plotted as a function of the mean count in a 25-ms interval for the Poisson process with constant deadtime. The deadtime was set equal to 2.0 ms, which is a representative value for best fits to data from several neurons. Note that the derivative becomes small and negative for large values of the mean. This is consistent with the values of $\Delta\sigma/\Delta m$ calculated for the unequal-variance Gaussian model of the receiver operating characteristics (see Tables I and II).

reciprocal of the best-fitting parameter for the exponentially distributed deadtime model was 2.0 ms. For neuron CH3308, these values were 2.1 and 2.3 ms, respectively. We have only analyzed some of our data in this way, but values around 2 ms seem representative.

As can be seen in Fig. 9, the predictions of the two models are similar for low spike counts but diverge for high spike counts. For the two neurons shown in Fig. 9, there is a tendency for the variance to decrease at the highest values of the mean. This decrease is consistent only with the constant-deadtime model. For all our data, the variance levels off at high mean rates and, for many cases, even decreases where high enough intensities were studied. For a few neurons with very high spontaneous rates, such as CH3225, the variance is roughly constant as the mean increases. In Fig. 10 the derivative of the standard deviation with respect to the mean, $d\sigma/dm$, is plotted as a function of the mean for the constant-deadtime model with 2-ms deadtime. Note that the derivative becomes small at high mean counts and that at even higher counts the derivative becomes negative. These values of $d\sigma/dm$ are consistent with the values of $\Delta\sigma/\Delta m$ given in Tables I and II for fits to our ROC data.

Therefore, the Poisson process with constant deadtime seems to be consistent with the statistics of responses to short tone bursts. The predictions of the two Poisson models differ most at the highest firing rates. For high mean counts, the variance decreases with the mean for the constant-deadtime model but continues to increase for the exponentially distributed deadtime model. The data of Teich and Khanna (1985) clearly show that the variance initially increases with the mean, and then becomes almost independent of the mean. However, in a few instances the variance did decrease for the highest mean counts. Young and Barta found that the exponentially distributed deadtime model provided a slightly better fit to their data, for which the variance continued to grow with the mean but with a decelerating rate. However, their data were restricted to average firing rates below 175 spikes/s. Similarly, Teich and Khanna (1985) only studied responses below 200 spikes/s. Delgutte's (1987) data include average firing rates up to 280 spikes/s. Here the variance becomes almost independent of the mean at high average rates but does not show the decrease sometimes seen in our data. Nonetheless, Delgutte chose to fit his data with a constant-deadtime model. We studied responses as high as 320 spikes/s and often found that the variance decreased at high mean counts. Since we never reached saturation, even higher firing rates are possible, which should allow a more critical test of the Poisson models. The reader should keep in mind that our data are for responses to 25-ms tone bursts. These responses include the large onset response. Therefore, the firing rate averaged over the duration of the tone burst is greater than that possible for the responses to long tone bursts or continuous tones. For these latter cases the average firing rate is dominated by the lesser steady-state response.

IV. CONCLUSIONS

The primary goal of these experiments was to verify a quick criterion-free method for measuring detectability in the auditory nerve. Such a method could then be used to study masking in the auditory nerve in a manner that allowed comparisons to behavioral experiments. The 2IFC task with an up–down procedure based on the PEST procedure has met that goal. The 2IFC thresholds with a standard deviation of 2.7 dB were measured in about 1 min. New up–down procedures, even more efficient than PEST, generally require even fewer trials for the same accuracy, and promise even quicker results (e.g., Hall, 1981; Watson and Pelli, 1983; Pelli, 1987). It is now possible to measure masking in the auditory nerve for many conditions within the usual recording time available for a single auditory neuron. These methods have been used to study forward masking of CF

tones by CF maskers, and the results will be presented in a forthcoming article (Relikin and Turner, 1987; Relkin and Turner, in preparation).

The 2IFC task yields data that allow construction of physiological ROC curves and neurometric functions that are directly comparable to animal and human psychophysical measures. We found that 2IFC neurometric functions were less steep than the most nearly comparable psychophysical functions. Physiological ROC curves had slopes much closer to 1 than the most nearly comparable psychophysical functions, and the ratio $\Delta\sigma/\Delta m$ was about 0.08, which is significantly less than the value of 0.25 often found psychophysically. These differences are consistent with the idea that the animal bases its psychophysical decision on the combination of many responses like the ones studied here.

Examination of pulse-number distribution statistics showed that, as the mean rate increases, the variance first increases, then peaks, and often finally decreases at very high mean rates. These results were most consistent with a 2-ms constant-deadtime Poisson model.

ACKNOWLEDGMENTS

This work was supported by grants from the Whitaker Foundation and the Deafness Research Foundation to one author, EMR. In the later stages, EMR was also supported by NIH Grant NS24255. The other author, DGP, was supported by NIH Grant EY04432. We thank an anonymous reviewer of a grant proposal to the Whitaker Foundation for comments that led to this line of research. We thank Eric Young for suggesting the test of the Poisson models, Christopher W. Turner, Clayton L. Van Doren, and Robert L. Smith for helpful discussion and suggestions, Michael A. Zaffuto of MAZ Audio for building the custom electronics that made this work possible, and Christos G. Stathatos, Jr. for performing surgical preparations.

APPENDIX: THE UNEQUAL-VARIANCE GAUSSIAN MODEL FOR ROC DATA

Conceptually the unequal-variance Gaussian model has four parameters: the mean μ_N and variance σ_N^2 of the decision variable on the no-probe ("noise only") interval, and the mean μ_{SN} and variance σ_{SN}^2 on the probe ("signal plus noise") interval. However, an ROC curve like that in Eq. (4) has only two degrees of freedom s and Δm, so we cannot determine the four parameters of the model. Recall that yes–no decisions are ideally made by comparing the decision variable with a criterion, which we shall represent as λ. For the Gaussian model the normal deviates z_N and z_{SN} are each the mean of the decision variable minus the criterion λ, normalized by the standard deviation of the decision variable,

$$z_N = (\mu_N - \lambda)/\sigma_N, \tag{A1}$$

$$z_{SN} = (\mu_{SN} - \lambda)/\sigma_{SN}. \tag{A2}$$

These two equations, parametrized in λ, describe a line when plotted in ROC space as z_N vs z_{SN} [e.g., Figs. 3(f) and 4(f)]. The slope s of that line is the ratio of the standard deviations, and the negative horizontal intercept Δm is the normalized difference of the means,

$$s = \sigma_N/\sigma_{SN}, \tag{A3}$$

$$\Delta m = (\mu_{SN} - \mu_N)/\sigma_N. \tag{A4}$$

Finally, $\Delta\sigma$ is the normalized difference between the standard deviations of the decision variable on signal-plus-noise and noise-only presentations,

$$\Delta\sigma = (\sigma_{SN} - \sigma_N)/\sigma_N = 1/s - 1. \tag{A5}$$

Barlow, H. B., and Levick, W. R. (**1969a**). "Three factors limiting the reliable detection of light by the retinal ganglion cells of the cat," J. Physiol. (London) **200**, 1–24.

Barlow, H. B., and Levick, W. R. (**1969b**). "Changes in maintained discharge with adaptation level in the cat retina," J. Physiol. (London) **202**, 699–718.

Barlow, H. B., Levick, W. R., and Yoon, M. (**1971**). "Responses to single quanta of light in retinal ganglion cells of the cat," Vision Res. **11** (Suppl. 3), 87–101.

Bauer, J. W. (**1978**). "Tuning curves and masking functions of auditory-nerve fibers in cat," Sen. Process. **2**, 156–172.

Delgutte, B. (**1987**). "Peripheral auditory processing of speech information: Implications from a physiological study of intensity discrimination," in *Psychophysics and Speech*, edited by M. E. H. Schouten (in press).

Dorfman, D. D., and Alf, E., Jr. (**1969**). "Maximum likelihood estimation of parameters of signal-detection theory and determination of confidence intervals: Rating method data," J. Math. Psychol. **6**, 487–496.

Emmerich, D. S. (**1968**). "Receiver-operating characteristics determined under several interaural conditions of listening," J. Acoust. Soc. Am. **43**, 298–307.

Geisler, C. D., Deng, L., and Greenberg, S. R. (**1985**). "Thresholds for primary auditory nerve fibers using statistically defined criteria," J. Acoust. Soc. Am. **77**, 1102–1109.

Goldstein, M. H., and Kiang, N. Y.-S. (**1958**). "Synchrony of neural activity in electrical responses evoked by transient acoustic stimuli," J. Acoust. Soc. Am. **30**, 107–114.

Green, D. M., and Swets, J. A. (**1966**). *Signal Detection Theory and Psychophysics, 1974 Edition* (Kreiger, New York).

Green, D. M., and Luce, R. D. (**1975**). "Parallel psychometric functions from a set of independent detectors," Psychol. Rev. **82**, 483–486.

Guinan, J. J., and Peake, W. T. (**1967**). "Middle-ear characteristics of anesthetized cats," J. Acoust. Soc. Am. **41**, 1237–1261.

Hack, M. H. (**1963**). "Signal detection in the rat," Science **139**, 758–759.

Hall, J. L. (**1981**). "A hybrid adaptive procedure for estimation of psychometric functions," J. Acoust. Soc. Am. **69**, 1763–1769.

Halpern, D. L. (**1985**). "Auditory filter shapes in the chinchilla: A behavioral investigation," Ph.D. Dissertation, Northwestern University, Evanston, IL.

Halpern, D. L., and Dallos, P. (**1986**). "Auditory filter shapes in the chinchilla," J. Acoust. Soc. Am. **80**, 765–775.

Harris, D. M., and Dallos, P. (**1979**). "Forward masking of auditory nerve fiber responses," J. Neurophysiol. **42**, 1083–1107.

Kiang, N. Y.-S., Watanabe, T., Thomas, E. C., and Clark, L. F. (**1965**). *Discharge Patterns of Single Fibers in the Cat's Auditory Nerve, M. I. T. Research Monograph No. 35* (Technology, Boston).

Kiang, N. Y.-S., Moxon, E. C., and Levine, R. A. (**1970**). "Auditory nerve activity in cats with normal and abnormal cochleas," in *Sensorineural Hearing Loss*, edited by G. E. W. Wolstenholme and J. Knight (Churchill, London), pp. 241–273.

Levitt, H. (**1971**). "Transformed up–down methods in psychoacoustics," J. Acoust. Soc. Am. **49**, 467–477.

Liberman, M. C. (**1978**). "Auditory-nerve response from cats raised in a low-noise chamber," J. Acoust. Soc. Am. **63**, 442–455.

Lütkenhöner, B., and Smith, R. L. (**1986**). "Rapid adaptation of auditory-nerve fibers: Fine structure at high stimulus intensities," Hear. Res. **24**, 289–294.

Markowitz, J., and Swets, J. A. (**1967**). "Factors affecting the slope of empirical ROC curves: Comparison of binary and rating responses," Percept. Psychophys. **2**, 91–97.

Movshon, J. A., Tolhurst, D. J., and Dean, A. F. (**1982**). "How many neurons are involved in perceptual decisions?," Invest. Ophthalmol. Vis. Sci. **22**, 207.

Nachmias, J., and Kocher, E. C. (**1970**). "Visual detection and discrimination of luminous increments," J. Opt. Soc. Am. **60**, 382–389.

Nelson, D. A., Kiester, T. E., Turner, C. W., and Ward, W. D. (**1976**). "Automated conditioned-avoidance audiometry in the chinchilla," J. Aud. Res. **16**, 209–237.
Nolte, L. W., and Jaarsma, D. (**1967**). "More on the detection of one of *M* orthogonal signals," J. Acoust. Soc. Am. **41**, 497–505.
Özdamar, Ö., and Dallos, P. (**1978**). "Synchronous responses of the primary auditory fibers to the onset of tone burst and their relation to compound action potentials," Brain Res. **155**, 169–175.
Parker, A., and Hawken, M. (**1985**). "Capabilities of monkey cortical cells in spatial-resolution tasks," J. Opt. Soc. Am. **A2**, 1101.
Pelli, D. G. (**1985**). "Uncertainty explains many aspects of visual contrast detection and discrimination," J. Opt. Soc. Am. **2**, 1508–1532.
Pelli, D. G. (**1987**). "The ideal psychometric procedure," Suppl. Invest. Ophthalmol. Vis. Sci. **28**, 366.
Peterson, W. W., Birdsall, T. G., and Fox, W. C. (**1954**). "Theory of signal detectability," IRE Trans. Inf. Theory **PGIT-4**, 171–212.
Quick, R. F. (**1974**). "A vector magnitude model of contrast detection," Kybernetik **16**, 65–75.
Relkin, E. M., and Turner, C. W. (**1987**). "Forward masking in auditory-nerve fibers," Abstracts of the Tenth Midwinter Meeting of the Association for Research in Otolaryngology, 233.
Salvi, R., Perry, J., Hamernik, R. P., and Henderson, D. (**1982**). "Relationships between cochlear pathologies and auditory nerve and behavioral responses following acoustic trauma," in *New Perspectives in Noise-Induced Hearing Loss*, edited by R. P. Hamernik, D. Henderson, and R. Salvi (Raven, New York), pp. 165–188.
Sinex, D. G., and Havey, D. C. (**1986**). "Neural mechanisms of tone-on-tone masking: Patterns of discharge rate and discharge synchrony related to rates of spontaneous discharge in the chinchilla auditory nerve," J. Neurophysiol. **56**, 1763–1780.
Smith, R. L. (**1977**). "Short-term adaptation in single auditory nerve fibers: Some poststimulatory effects," J. Neurophysiol. **49**, 1098–1112.
Smith, R. L. (**1979**). "Adaptation, saturation, and physiological masking in single auditory-nerve fibers," J. Acoust. Soc. Am. **65**, 166–178.
Swets, J. A., and Pickett, R. M. (**1982**). *Evaluation of Diagnostic Systems, Methods from Signal Detection Theory* (Academic, New York).
Tanner, W. P., Jr., and Swets, J. A. (**1954**). "A decision-making theory of visual detection," Psychol. Rev. **61**, 401–409.
Taylor, M. M., and Creelman, C. D. (**1967**). "PEST: Efficient estimates of probability functions," J. Acoust. Soc. Am. **41**, 782–787.
Teich, M. C., and Khanna, S. M. (**1985**). "Pulse-number distribution for the neural spike train in the cat's auditory nerve," J. Acoust. Soc. Am. **77**, 1110–1128.
Tolhurst, D. J., Movshon, J. A., and Dean, A. F. (**1983**). "The statistical reliability of signals in single neurons in cat and monkey visual cortex," Vision Res. **23**, 775–785.
Van Trees, H. L. (**1968**). *Detection, Estimation, and Modulation Theory* (Wiley, New York).
Watson, A. B. (**1979**). "Probability summation over time," Vision Res. **19**, 515–522.
Watson, A. B., and Pelli, D. G. (**1983**). "QUEST: A Bayesian adaptive psychometric method," Percept. Psychophys. **33**, 113–120.
Watson, C. S., Franks, J. R., and Hood, D. C. (**1972**). "Detection of tones in the absence of external masking noise. I. Effects of signal intensity and signal frequency," J. Acoust. Soc. Am. **52**, 633–643.
Weibull, W. (**1951**). "A statistical distribution function of wide applicability," J. Appl. Mech. **18**, 292–297.
Westerman, L. A. (**1985**). "Adaptation and Recovery of Auditory Nerve Responses," Ph.D. dissertation, Syracuse University, Syracuse, NY.
Young, E. D., and Barta, P. E. (**1986**). "Rate response of auditory nerve fibers to tones in noise near masked threshold," J. Acoust. Soc. Am. **79**, 426–442.
Zwislocki, J., Maire, F., Feldman, A. S., and Rubin, H. (**1958**). "On the effect of practice and motivation on the threshold of audibility," J. Acoust. Soc. Am. **30**, 254–262.